LA-UR- 11-02219

Approved for public release; distribution is unlimited.

Title: An Evaluation of the Attila™ Transport Code as a Tool for Use by the Los Alamos National Laboratory Radiological Engineering Group

Author(s): Daniel A. Gonzalez
Garry R. Schramm

Intended for: Public Release

Los Alamos NATIONAL LABORATORY EST.1943

1 INTRODUCTION

The Radiological Engineering Team in conjunction with the AET-2 organization (Process Modeling and Analysis) investigated the functionality of Attila™ for the rapid evaluation of ergonomic driven glovebox design modifications on worker dose.

Attila™ provides a design based environment for radiation transport simulations. It combines deterministic radiation transport analysis with intuitive and integrated processes from computer aided engineering (CAE) disciplines. The primary goal in the development of Attila™ was to provide a modeling tool which increases productivity, enabling analysts to spend less time on setting up and running calculations.

Attila™ provides the following features:

- No variance reduction required
- Direct import from leading CAD systems
- Intuitive graphical user interface
- Conformal modeling of complex geometry
- Neutral, charged, and coupled particle support
- Solution obtained everywhere in the domain

This investigation was motivated by the need to quickly and accurately evaluate the effect on worker doses from proposed changes, or analyze multiple options, as in the case of changes to glovebox designs in order to minimize ergonomic injuries of glovebox workers. The complexity of these analyses has required a significant amount of up-front time by highly knowledgeable analysts to model the physical geometry of the glovebox, associated equipment, and the radioactive source.

Based on Attila's™ advertised features, its use may produce efficiencies in the modeling and analysis of glovebox ergonomic design features and allow for a more timely and cost effective exploration of design options.

The primary focus of this evaluation is twofold: to explore Attila's CAD import capability as a means to reduce the time and cost in evaluating new designs for compliance with worker dose regulations; and, to evaluate Attila's ability to yield accurate results.

The evaluation was accomplished by acquiring a CAD design of a PF-4 glovebox from a local A&E firm, importing the design into Attila™, and comparing results obtained against measured dose rates from radioactive material placed in the PF-4 glovebox. The LANL RP-2 organization assisted this effort by taking the required measurements around the PF-4 glovebox using a combination of dosimeters and radiation detection instrumentation. Lastly, the source and glovebox were modeled, and dose rates calculated, using MCNP. These results were compared to those obtained from measured data and from Attila™.

2 PROJECT INFORMATION

A single station glovebox was used in this evaluation. Figure 1 displays a three dimensional CAD model of the glovebox. Solidworks© was used to generate the three dimensional model of the glovebox and the dosimetry phantom used in this evaluation.

The glovebox was loaded with neutron/gamma emitting source material. A dosimetry phantom was placed in front of the glovebox and several thermoluminescent dosimeters were attached to the phantom. Dosimeters were attached to the phantom inside the glovebox to obtain extremity measurements and outside of the glovebox on the phantom to obtain doses associated with whole body irradiation. Figure 2 displays a three dimensional CAD model of the phantom used. The phantom's arms and main body are made of Lucite. The support structure is made of stainless steel.

Figure 3 displays the single station glovebox and phantom in position. Dosimeters were positioned in front and behind the Lucite main body as well as on the arms that extend into the glovebox.

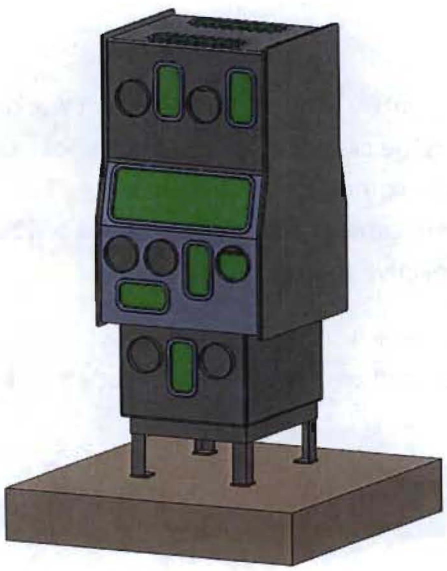

Figure 1 – Single Station Glovebox

Figure 2 – Phantom

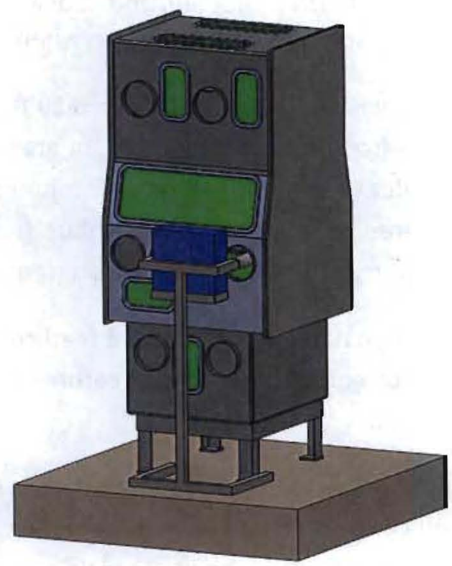

Figure 3 – Glovebox and Phantom

Nineteen cans filled with varying quantities of photon and neutron-emitting nuclear material were positioned inside the glovebox. The spectra and source strength are discussed in the Source Term section of this report. The 19 cans were placed within the main workspace of the glovebox. The 19 can source in relation to the dosimetry phantom is shown in Figure 4.

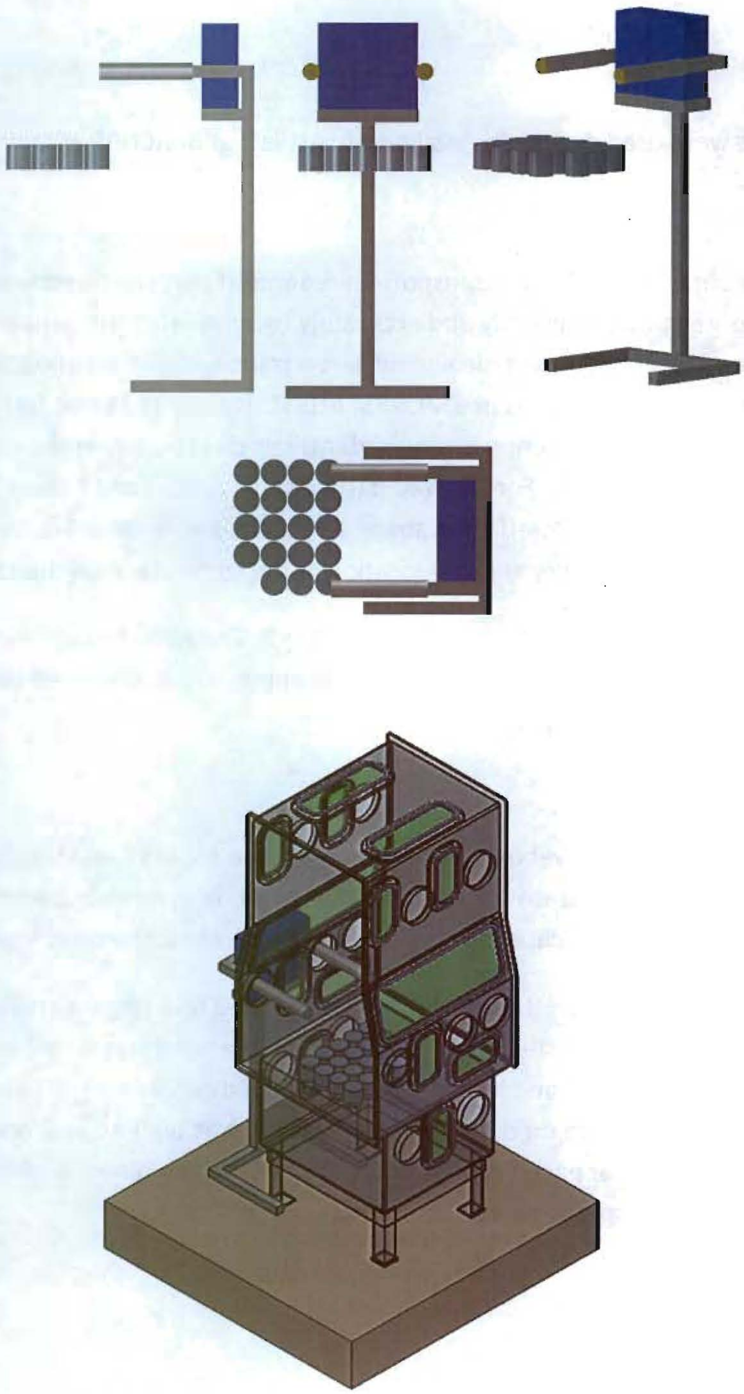

Figure 4 – Several Views of the 19 Can Radiation Source and the TLD Phantom

3 CODES

Two transport codes were used during this evaluation: Attila™ and MCNP5.

3.1 Attila™

Attila™ is a deterministic radiation transport environment that can directly use CAD data and model complex geometry efficiently and accurately to solve large 3-D problems. Attila™ can solve for neutron, gamma, charged particle and infra-red transport and accounts for the same transport effects as Monte Carlo type codes like MCNP5. Attila™ is reported to be faster than Monte Carlo methods and no variance reduction is required. Attila™ directly solves the differential form of the Boltzmann transport equation. For charged particles, the Boltzmann-Fokker-Planck transport equation is solved. Attila™ discretizes in space, angle and energy to solve for flux as a function of angle, energy and particle type, at every location in the computational domain.

The Solidworks model was directly provided to Attila™. The Attila™ code was then able to use the information provided to generate dose rates at all points within the three dimensional model defined by the Solidworks model.

3.2 MCNP5

A simplified model of the glovebox was created using the Monte Carlo transport code developed by Los Alamos National Laboratory – MCNP5. The glovebox as modeled with MCNP5 is shown in Figure 5, which also shows a cutaway of the glovebox to reveal the source within.

The MCNP source term within the glovebox was simplified to a single parallelepiped encased within a 1 mm thick stainless steel outer shell. The source term was distributed throughout the red shape shown on Figure 5 and its density was adjusted accordingly. There are notable differences between the two models. The MCNP model was built as a secondary check of the expected dose response at each location of interest and to examine the effect of simplifying the glovebox and source term geometry.

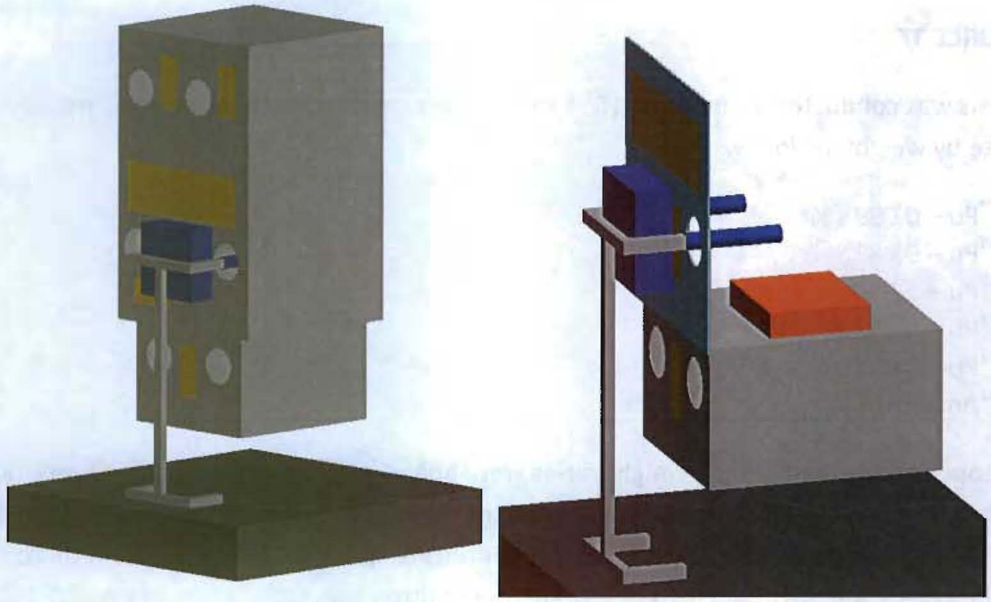

Figure 5 – Two Views of an MCNP Model of the Single Station Glovebox

4 SOURCE TERM

The analysis was conducted assuming 4.1653 kg of nuclear material with an isotopic mixture, given in percentage by weight, as follows:

- ^{238}Pu – 0.0993 %
- ^{239}Pu – 93.82 %
- ^{240}Pu – 5.95 %
- ^{241}Pu – 0.198 %
- ^{242}Pu – 0.02 %
- ^{241}Am – 0.16 %

These isotopes and corresponding weight ratios were analyzed using Lawrence Livermore National Laboratory's (LLNL) code RadSrc, which calculates the isotopic mixture present after a specified decay period, as well as the resulting photon energy and intensity spectra. The output from this code is used as input to the LANL code SOURCES4c to determine the neutron spectrum information. SOURCES4c provided the neutron energy spectra and intensity from the spontaneous fission of ^{240}Pu.

Attachment 1 displays the neutron spectra used in the analysis. The entirety of neutrons emissions arise from the spontaneous fission of Pu. Attachment 2 displays the photon energy spectra.

The source was distributed over 19 cans positioned within the glovebox as shown in Figure 4. The distribution of material is shown in Table 1 – Distributed Source Quantities.

Table 1 – Distributed Source Quantities

Can #	Source Material (g)	Can #	Source Material (g)
1	374.4	11	168.0
2	283.0	12	499.2
3	168.2	13	129.1
4	99.5	14	158.3
5	171.6	15	146.5
6	117.0	16	457.2
7	146.6	17	126.0
8	481.4	18	154.3
9	161.4	19	118.2
10	205.4	Total	4165.3

5 RESULTS

The single station glovebox measured and calculated results are reported for two exposure periods and two locations: 23.25 and 145.25 hour exposures, and front and back of the glovebox. The results are provided in Tables 2 through 4. Each of these tables displays a measurement location identifier corresponding to its X Y Z coordinate location. It also shows the type and identifying number for each dosimeter used, and the location in space where it was deployed. The location in space is relative to the center of the top of the can located on the first row, first position from the left.

Three columns of data follow the X Y Z positions. The first column following the positions displays the measured photon and neutron results (γ and n). Thermoluminescent (TLD), extremity (EXT) and electronic pocket dosimeters (EPD) were used to collect the measured photon and neutron data. The next column labeled Attila™ (mrem) displays the photon and neutron results calculated by the Attila™ code. The MCNP5 photon and neutron results are displayed in the column labeled MCNP (mrem).

Figure 6 shows a top down view of the TLD phantom along with the 19 cans of source material. The origin relative to the X Y Z positions indicated on Tables 2 through 4 is shown in Figure 6 as a black dot on a red can. Figure 7 displays the measurement locations relative to the phantom and source.

Table 2 displays Measured, Attila™ and MCNP photon and neutron results of the 23.25 hour exposure period; front position. Figure 8 displays photon dose results and Figure 9 displays neutron dose results of the Table 2 data.

Table 3 displays Measured, Attila™ and MCNP photon and neutron results of the 145.25 hour exposure period; front location. Figure 10 displays photon dose results and Figure 11 displays neutron dose results of the Table 3 data.

Table 4 displays Measured and Attila™ results of the 23 hour exposure period; back location. MCNP results were not calculated for the back location. Figure 12 displays photon dose results and Figure 13 displays neutron dose results of the Table 4 data.

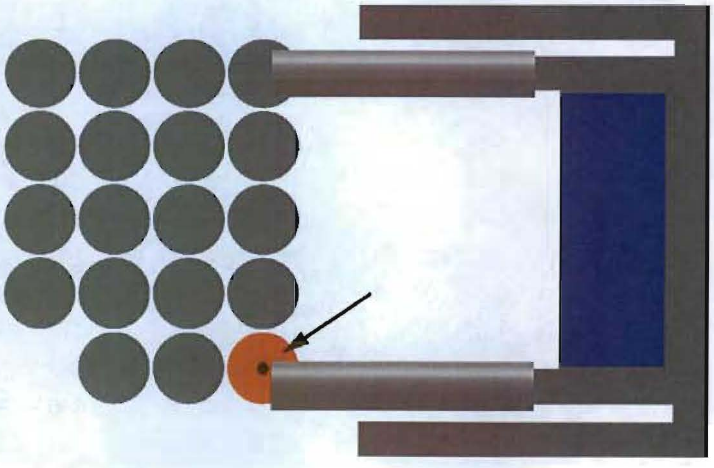

Figure 6 – Coordinate System Origin (0, 0, 0 cm)

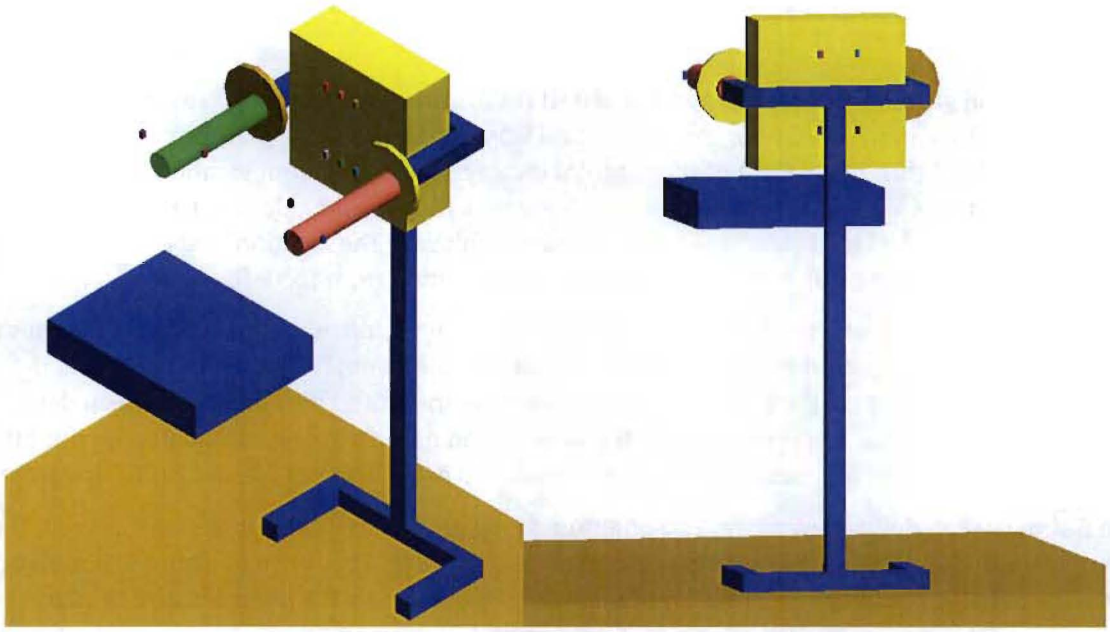

Figure 7 – Measurement Locations

Table 2 – Glovebox Front Results for 23.25-hour Exposure Period

Jan 27 - 28 Exposure - 23.25 hrs											
Measurement Location	Dosimeter Type and ID	Location (cm)			Measured (mrem)		Attila (mrem)		MCNP (mrem)		Comment
		x	y	z	γ	n	γ	n	γ	n	
1	TLD -37568	40.64	15.24	40.64	150	37	190	27	180	20	Phantom, front
2	TLD -37812	40.64	15.24	20.32	172	0	253	38	210	27	Phantom, front
3	TLD -37992	40.64	25.40	40.64	123	51	227	31	176	20	Phantom, front
4	TLD -37975	40.64	25.40	20.32	168	48	309	43	222	28	Phantom, front
5	TLD -37956	60.96	15.24	40.64	18	0	28	1.3	22	0.9	Phantom, back
6	TLD -37897	60.96	15.24	20.32	17	6	22	2.4	20	1.7	Phantom, back
7	TLD -37980	60.96	25.40	40.64	21	10	24	1.3	20	0.9	Phantom, back
8	TLD -37816	60.96	25.40	20.32	19	10	19	2.3	20	1.7	Phantom, back
9	EPD-010362	40.64	20.32	40.64	191	17	210	29	202	20	Phantom, front EPD
10	EPD-010367	40.64	20.32	20.32	163	35	308	42	257	28	Phantom, front EPD
11	EXT -19838	5.08	-7.62	30.48	485	0	370	38	416	28	Arm, outside L
12	EXT -19839	10.16	7.62	30.48	645	0	470	49	567	39	Arm, inside L
13	EXT -19840	5.08	53.34	30.48	822	141	445	52	440	33	Arm, outside R
14	EXT -19841	10.16	38.10	30.48	525	0	541	57	569	40	Arm, inside R

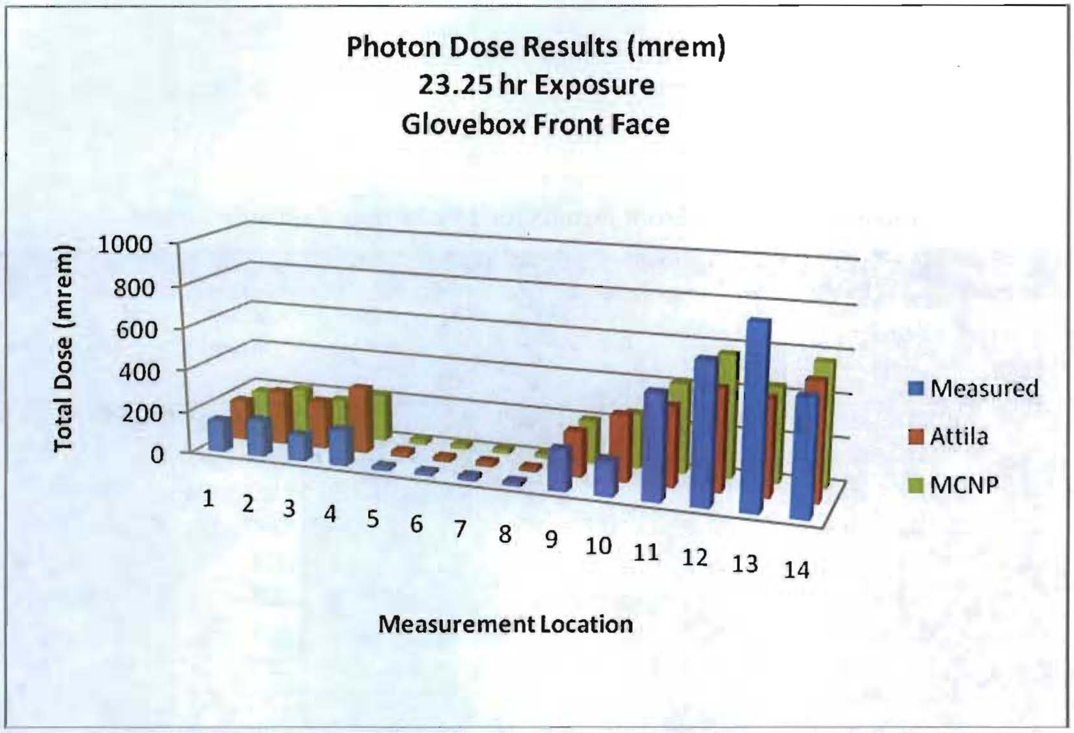

Figure 8 – Jan 27 -28 Glovebox Front Photon Dose Results

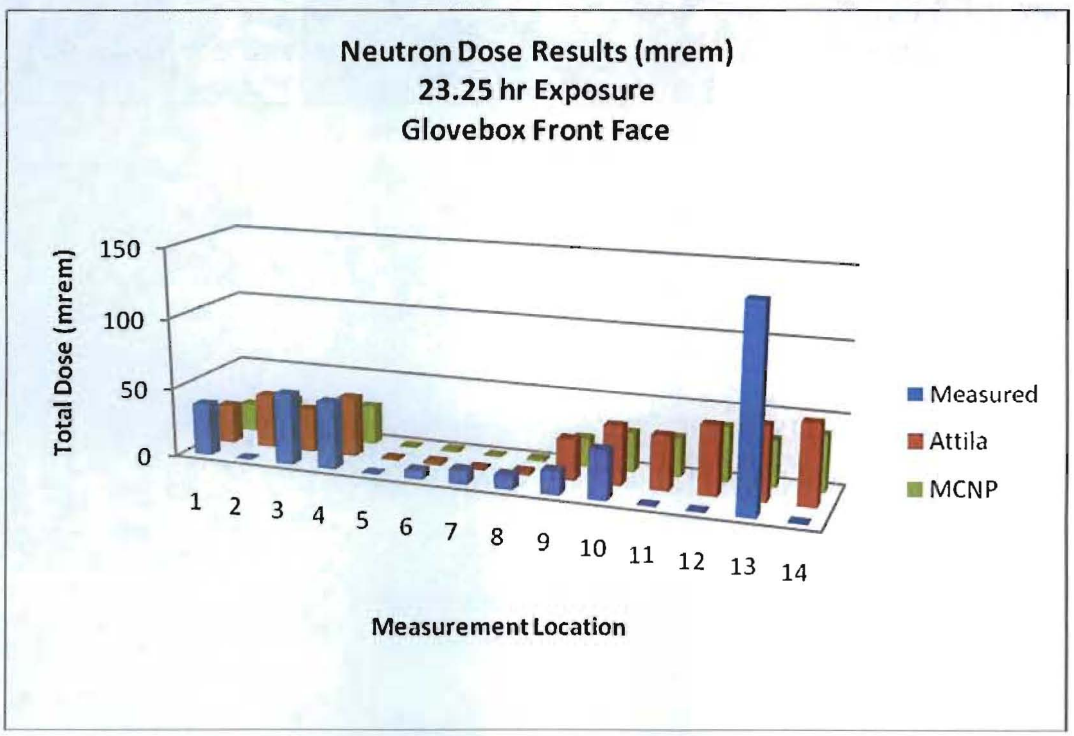

Figure 9 - Jan 27 -28 Glovebox Front Neutron Dose Results

Table 3 – Glovebox Front Results for 145.25-hour Exposure Period

Jan 29 - Feb 04 Exposure - 145.25 hrs											
Measurement Series	***Dosimeter Type and ID***	***Location (cm)***			***Measured (mrem)***		***Attila (mrem)***		***MCNP (mrem)***		***Comment***
		x	***y***	***z***	***γ***	***n***	***γ***	***n***	***γ***	***n***	
3	TLD -36336	40.64	15.24	40.64	823	0	1185	171	1124	125	Phantom, front
3	TLD -36922	40.64	15.24	20.32	951	124	1581	240	1314	171	Phantom, front
3	TLD -36753	40.64	25.40	40.64	824	140	1418	191	1102	124	Phantom, front
3	TLD -36899	40.64	25.40	20.32	952	149	1930	268	1387	173	Phantom, front
3	TLD -36810	60.96	15.24	40.64	122	47	176	8	137	5	Phantom, back
3	TLD -36790	60.96	15.24	20.32	119	59	134	15	123	11	Phantom, back
3	TLD -36359	60.96	25.40	40.64	137	53	149	8	125	6	Phantom, back
3	TLD -38435	60.96	25.40	20.32	138	53	118	14	126	11	Phantom, back
3	EPD 010362	40.64	20.32	40.64	1220	118	1314	180	1261	127	Phantom, front EPD
3	EPD 010367	40.64	20.32	20.32	1390	223	1922	261	1605	175	Phantom, front EPD
3	EXT -20178	5.08	-7.62	30.48	4455	0	2314	238	2596	173	Arm, outside L
3	EXT -20179	10.16	7.62	30.48	6483	0	2933	305	3544	244	Arm, inside L
3	EXT -20176	5.08	53.34	30.48	4107	1734	2781	327	2750	205	Arm, outside R
3	EXT -20177	10.16	38.10	30.48	9440	0	3378	355	3552	248	Arm, inside R

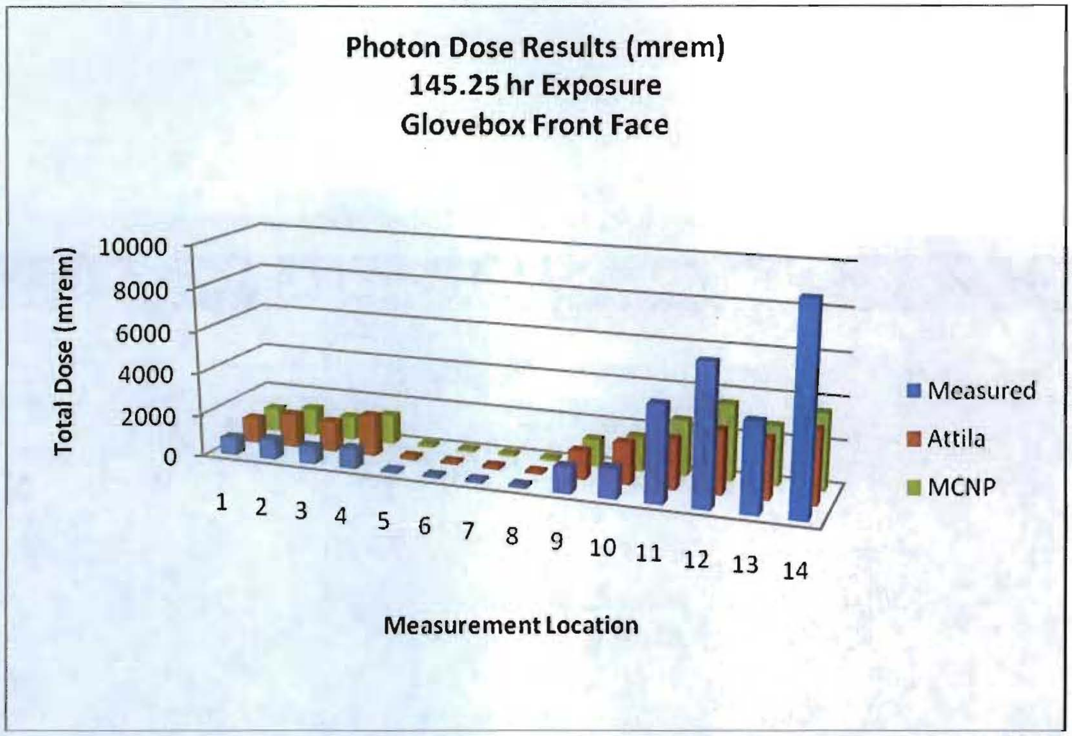

Figure 10 – Jan 29 –Feb 4 Glovebox Front Photon Dose Results

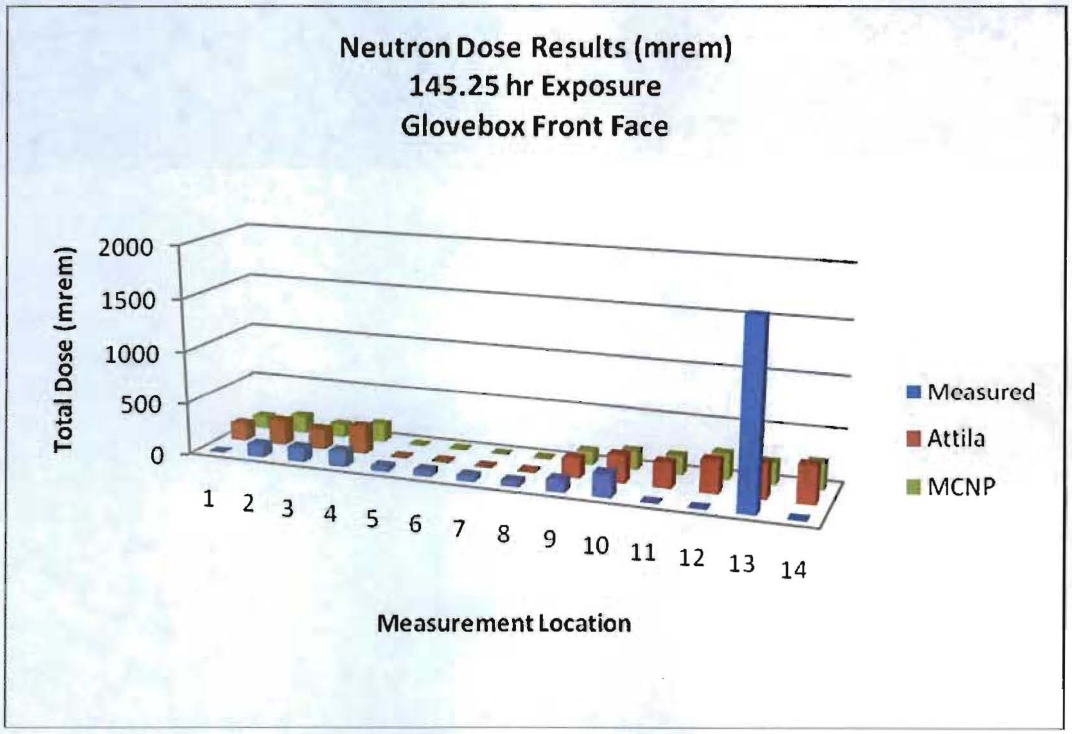

Figure 11 – Jan 29 –Feb 4 Glovebox Front Neutron Dose Results

Table 4 – Glovebox Back Results for 23-hour Exposure Period

Jan 28 - 29 Exposure - 23 hrs									
Measurement Series	***Dosimeter Type and ID***	***Location (cm)***			***Measured (mrem)***		***Attila (mrem)***		***Comment***
		x	***y***	***z***	***γ***	***n***	***γ***	***n***	
2	TLD -36399	-71.12	15.24	40.64	116	15	118	17	Phantom, front
2	TLD -36833	-76.20	15.24	20.32	138	22	113	21	Phantom, front
2	TLD -94012	-71.12	25.40	40.64	140	0	137	20	Phantom, front
2	TLD -38679	-76.20	25.40	20.32	146	0	128	22	Phantom, front
2	TLD -36358	-91.44	15.24	40.64	34	13	70	11	Phantom, back
2	TLD -36815	-96.52	15.24	20.32	50	13	36	11	Phantom, back
2	TLD -36372	-91.44	25.40	40.64	40	20	70	12	Phantom, back
2	TLD -36935	-96.52	25.40	20.32	36	0	34	10	Phantom, back
2	EPD 010362	-71.12	20.32	40.64	148	20	112	16	Phantom, front
2	EPD 010367	-76.20	20.32	20.32	116	24	119	18	Phantom, front
2	EXT -19849	-38.10	-7.62	30.48	963	0	282	32	Arm, outside L
2	EXT -19850	-43.18	7.62	30.48	486	0	319	35	Arm, inside L
2	EXT -19848	-38.10	53.34	30.48	503	0	304	37	Arm, outside R
2	EXT -19851	-43.18	38.10	30.48	567	0	334	37	Arm, inside R

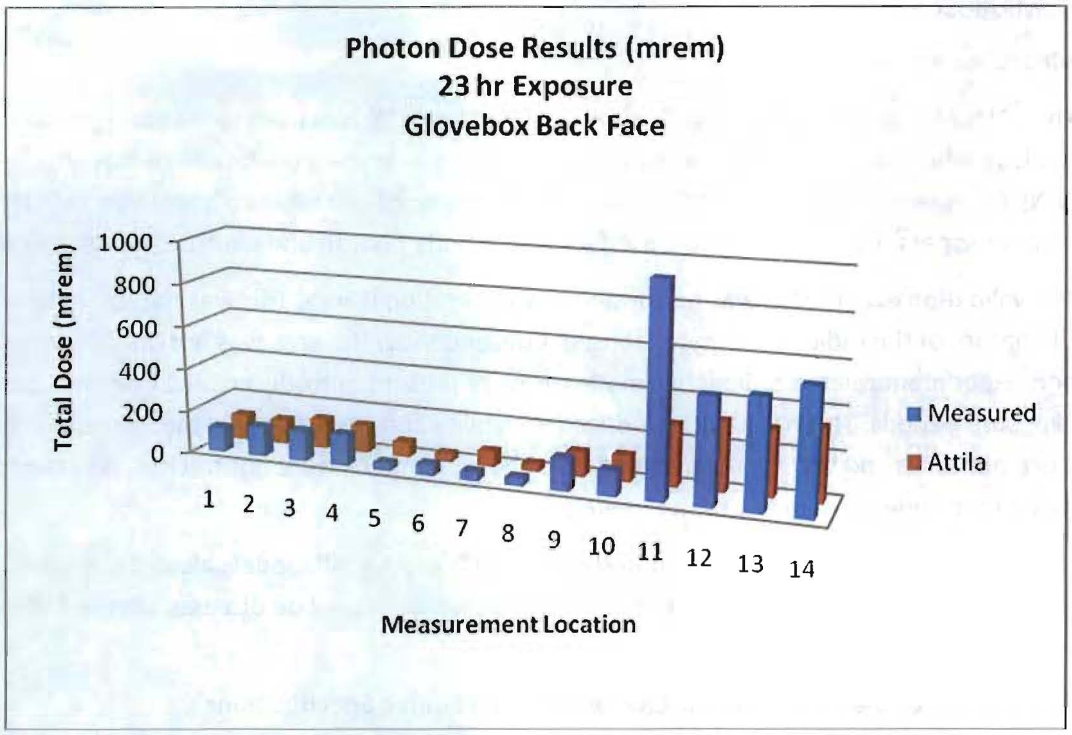

Figure 12 – Jan 29 –Feb 4 Glovebox Back Photon Dose Results

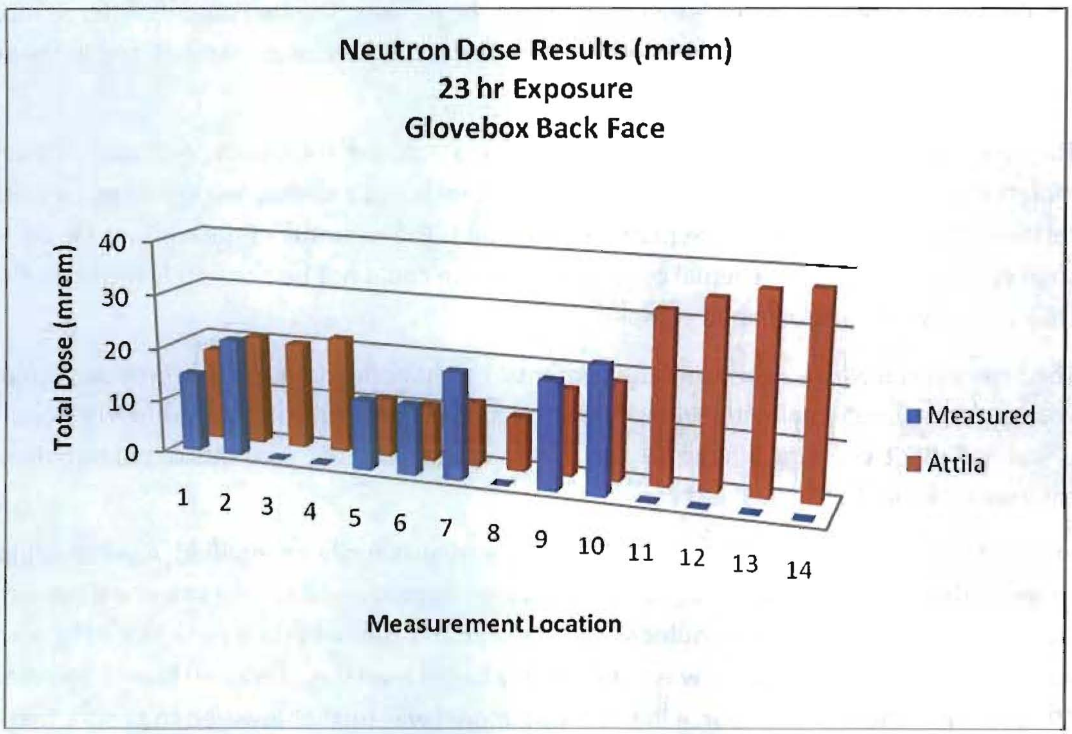

Figure 13 – Jan 29 –Feb 4 Glovebox Back Neutron Dose Results

6 COMPARISON

6.1 Measured Results

The LANL Model 8823 Thermoluminescent Dosimeter (TLD) was used to measure photon and neutron whole-body dose. Extremity measurements inside the glovebox were made using the LANL Comprehensive Extremity Dosimeter (EXT). ThermoFisher Scientific's Model EPD-Ns electronic personal dosimeter was used for whole body photon and neutron measurements.

The validation experiment was performed in an operational area. This was necessary because of the nature of the radioactive material used. Consequently, the area was not under control, and non-experiment related radioactive materials were present, introduced, and removed during the exposure periods. This naturally introduced variability and uncertainty in the measured results. Since materials and their positions relative to the experiment were not tracked, no attempt was made to include them in any of the models.

Even with the potential variability noted, the Attila™ and MCNP model calculations were reasonably accurate when compared to measured results as will be discussed in the following sections.

6.2 Comparison of the Attila™ and MCNP Models and Source Specifications

The data shows that there is generally good agreement between the measured, Attila™ and MCNP results, despite the obvious differences between the models. The two models differed most in the geometric shape and the calculated effective densities of the source material, and in the shape and details of the glovebox.

The source of radiation is fairly accurate in the Attila™ model. It consists of 19 cans of true size and material makeup. Each can has a 1 mm stainless steel body, a slightly thicker lid and a volume relative to the quantity of source material contained. The contents of the can were modeled as a solid cylindrical object. The actual contents of the can could not be accurately modeled since their true shapes were unknown and complex.

The heaviest can was weighed and the contents' height approximated. This provided a mass and volume from which an effective density was calculated and applied to the source material cylindrical shape contained in the 19 cans. This assumed that the contents of the remaining 18 cans were similar to the heaviest can.

In the case of the MCNP model, the source geometry was further simplified. A parallelepiped shape in the dimensions of the combined cans was created and encased in a one millimeter stainless steel outer shell. This outer shell simulated the stainless steel cans. Since the source volume in the MCNP geometry was considerably larger than the combined source volume of the 19 cans, the density of the source in the MCNP model was further lowered to ensure that the total mass of 4.1653 Kg was preserved.

Another significant difference between the models was in the shape of the glovebox frame. As can be noted by examining Figures 3 and 5, the MCNP model does not display the slanted viewing surface on either side. There is a further lack of details in the MCNP model regarding the viewports and gloveports. There are no materials covering the gloveports in the MCNP model as compared to the Hypalon gloveport covers applied in the Attila™ model. While the MCNP model viewports are covered in the same glass, it does not display viewport and gloveport casings as does the Attila™ model.

6.3 Comparison of Measured and Calculated Results

The null hypothesis when testing for differences is typically stated as no difference between the two groups under consideration. This may be written as: H_0: $\mu_1 = \mu_2$. Since the points in space chosen for this evaluation differ in dose rates (and consequently in total dose), the ratio of the measured to calculated results were considered. The null hypothesis equation can be rearranged to become H_0: $\mu_1 / \mu_2 = 1$. For these evaluations, the null hypothesis is that the mean of the ratios is equal to 1.

For normally distributed data, a one sample *t*-test can be used to check the ratios of any two sets of data against the underlying mean ratio of 1.000. If the ratios appear skewed, or not normally distributed, then the log of the ratios will be examined and tested against the underlying mean ratio equal to zero.

6.3.1 Photon Results

6.3.1.1 Attila™ to Measured Comparison

The ratio of Attila™ to measured photon results for all points sampled ranged from 0.3 to 2.1. The mean of the ratios is 1.103 with one standard deviation at 0.477. Figure 14 displays a histogram of the ratios of Attila™ to Measured.

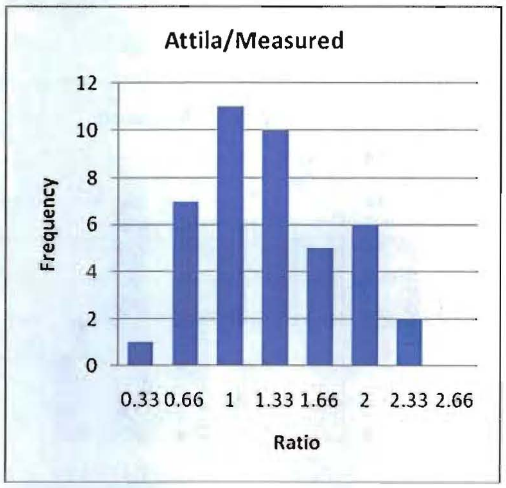

Figure 14 – Histogram of Attila™to Measured Photon Ratios

Of the 42 points sampled, 67% of the ratios fell between 0.66 and 1.33. The Kolmogorov-Smirnov test of normality finds the data consistent with a normal distribution: P=0.31 where the normal distribution has a mean equal to 1.136 and standard deviation of 0.4757. Assuming the data are normal; a one sample *t*-test provides the following information:

P value and statistical significance:
The two-tailed P value equals 0.1670
By conventional criteria, this difference is considered to be not statistically significant.

Confidence interval:
The hypothetical mean is 1.00
The actual mean is 1.103
The difference between these two values is 0.103
The 95% confidence interval of this difference:
From -0.045 to 0.252

Intermediate values used in calculations:
t = 1.4069
df = 41
standard error of difference = 0.074

It is concluded that when considering the ratio of Attila™ calculated photon results against the measured photon results; we cannot reject the null hypothesis that the underlying mean ratio is 1.0. This confirms that Attila™ has done a good job of estimating the actual measured photon dose rates.

6.3.1.2 MCNP to Measured Comparison

In comparison, the ratio of MCNP to measured photon results for all points sampled ranged from 0.38 to 1.6. The mean of the ratios of MCNP to Measured is 1.051 with 0.305 as one standard deviation. Figure 15 displays a histogram of the ratios of MCNP to Measured.

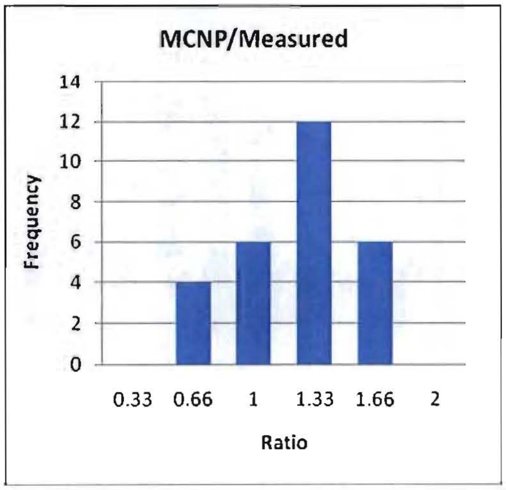

Figure 15 – Histogram of MCNP to Measured Photon Ratios

Of the 28 points sampled, 78% of the ratios fell between 0.66 and 1.33. The Kolmogorov-Smirnov test of normality finds the data consistent with a normal distribution: P=0.56 where the normal distribution has a mean equal to 1.031 and standard deviation of 0.3453. Assuming the data are normal; a one sample *t*-test provides the following information:

P value and statistical significance:
The two-tailed P value equals 0.3806
By conventional criteria, this difference is considered to be not statistically significant.

Confidence interval:
The hypothetical mean is 1.00
The actual mean is 1.051
The difference between these two values is 0.051
The 95% confidence interval of this difference:
From -0.06689704893 to 0.16968634093

Intermediate values used in calculations:
t = 0.8915
df = 27
standard error of difference = 0.058

It can again be concluded that when comparing the photon measured results against the MCNP calculated results; we cannot reject the null hypothesis that the underlying mean ratio is 1.0. This confirms that MCNP has also done a good job of estimating the actual measured photon dose rates.

6.3.1.3 MCNP to Attila™ Comparison

The ratio of MCNP to Attila™ photon results for all points sampled ranged from 0.72 to 1.2. The average of the ratios of MCNP to Attila™ is 0.93 with one standard deviation of the mean at 0.14. Figure 16 displays a histogram of the ratios of MCNP to Attila.

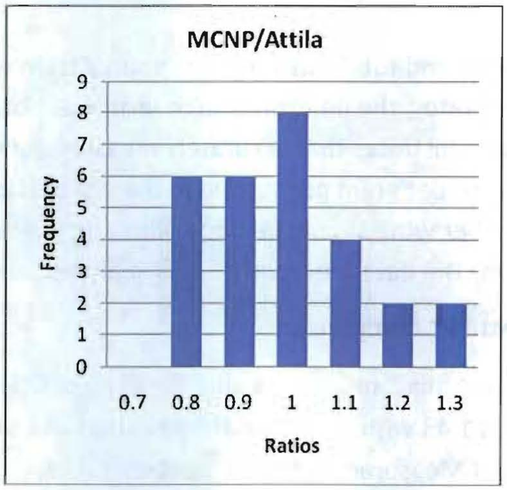

Figure 16 – Histogram of MCNP to Attila™Photon Ratios

The Kolmogorov-Smirnov test of normality finds the data consistent with a normal distribution: P=0.25 where the normal distribution has a mean equal to 0.942 and a standard deviation of 0.146. Assuming the data are normal; a one sample *t*-test provides the following information:

P value and statistical significance:
The two-tailed P value equals 0.0163
By conventional criteria, this difference is considered to be statistically significant.

Confidence interval:
The hypothetical mean is 1.000
The actual mean is 0.931
The difference between these two values is -0.0685
The 95% confidence interval of this difference:
From -0.12334150974 to -0.01367036426

Intermediate values used in calculations:
t = 2.5633
df = 27
standard error of difference = 0.027

The *t*-test result of this comparison is significant. We can conclude that when comparing the MCNP results to the Attila™ results, we *can* reject the null hypothesis that the underlying mean is equal to 1.

This indicates that the two models are not providing photon results comparable to each other, while providing photon results that are comparable to the measured data. This suggests that the differences in the two models noted in section 6.2 are significant. More work should be done to minimize the differences between the two models if there is interest in pursuing this aspect of the evaluation.

6.3.2 Neutron Results

While the photon intensity and total activity of the source term was sufficient to generate measurable photon dose rates, the neutron source term was not. The evaluation of the neutron results in this section demonstrates that accurately measuring a neutron source emitting approximately 63 neutrons per gram per second in the physical environment of a shielded glovebox is difficult. Further work should be done with a stronger neutron source term to complete this evaluation. The data are nevertheless analyzed below.

6.3.2.1 Measured to Attila™ Comparison

The ratio of Measured to Attila™ neutron results for all points sampled ranged from 0 to 7.72. The mean of the ratios is 1.43 with one standard deviation at 1.98. Figure 17 displays a histogram of the ratios of Measured to Attila™ neutron ratios.

The Kolmogorov-Smirnov test of normality finds that the data are not normally distributed with P=0.00 where the normal distribution has a mean of 2.38 and a standard deviation of 2.18. Furthermore, Tukey's test on outliers identifies the ratios of 4.42 through 7.72 as outliers.

The mean of the log of the ratios of the measured results compared to the Attila™ results is 0.08 with a standard deviation of 0.26. Ratios of 0 could not be evaluated in this manner and Tukey's recommendation to exclude the outliers was accepted. This reduced the useful data from 42 samples to 21. The results of the *t*-test are as follows:

P value and statistical significance:

The two-tailed P value equals 0.1739

By conventional criteria, this difference is considered to be not statistically significant.

Confidence interval:

The hypothetical mean is 0.0000

The actual mean is 0.0800

The difference between these two values is 0.0800

The 95% confidence interval of this difference:

From -0.0384 to 0.1984

Intermediate values used in calculations:

t = 1.4100

df = 20

standard error of difference = 0.057

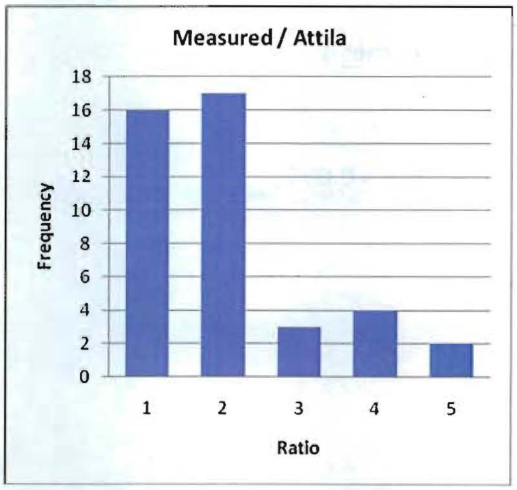

Figure 17 – Histogram of Measured to Attila™Neutron Ratios

It is concluded that when comparing the measured neutron results (excluding zeros and outliers) against the Attila™ calculated results we cannot reject the null hypothesis that the underlying mean of the log of the ratios is 0.0. While this suggests agreement between these two data sets, the overall validity of this test is questionable considering the number of unusable results.

6.3.2.2 Measured to MCNP Comparison

The ratio of Measured to MCNP neutron results for all points sampled ranged from 0.0 to 11.2. The mean of the ratios is 2.7 with 3.34 as one standard deviation. Figure 18 displays a histogram of the ratios of MCNP to Measured neutron ratios. The Kolmogorov-Smirnov test of normality finds the data are not normally distributed.

The mean of the log of the ratios of the measured results compared to the MCNP results is 0.43 with a standard deviation of 0.41. Ratios of 0 could not be evaluated in this manner. This reduced the useful data from 28 samples to 19. The results of the *t*-test are as follows:

P value and statistical significance:
The two-tailed P value equals 0.0002
By conventional criteria, this difference is considered to be statistically significant.

Confidence interval:
The hypothetical mean is 0.0000
The actual mean is 0.4300
The difference between these two values is 0.4300
The 95% confidence interval of this difference:
From 0.2324 to 0.6276

Intermediate values used in calculations:
t = 4.5715
df = 18
standard error of difference = 0.094

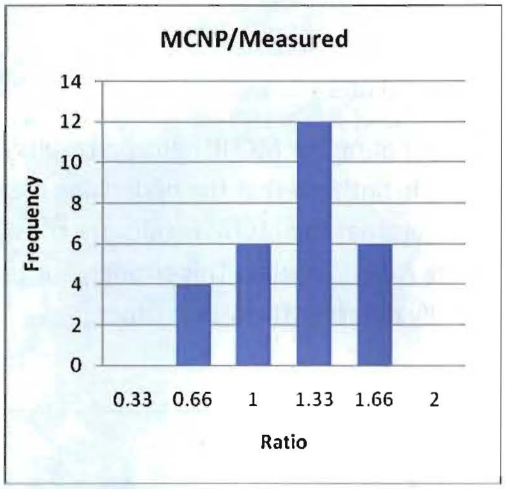

Figure 18 – Histogram of MCNP to Measured Neutron Ratios

We may conclude that when comparing the measured neutron results (excluding zeros and outliers) against the MCNP calculated results; we can reject the null hypothesis that the underlying mean of the log of the ratio is 0.0. Again we see potential evidence of a measurable difference between the models. The overall usefulness of this analysis is also questionable because of the number of outliers and zero results.

6.3.2.3 MCNP to Attila™ Comparison

The ratio of MCNP to Attila™ neutron results for all points sampled ranged from 0.63 to 0.80. The average of the ratios of MCNP to Attila™ is 0.70 with one standard deviation of the mean at 0.05. Figure 19 displays a histogram of the ratios of MCNP to Attila™.

The Kolmogorov-Smirnov test of normality finds the data consistent with a normal distribution: P=0.57 where the normal distribution has a mean equal to 0.705 and a standard deviation of 0.051. The results of the *t*-test are as follows:

<u>P value and statistical significance:</u>
The two-tailed P value is less than 0.0001
By conventional criteria, this difference is considered to be statistically significant.

<u>Confidence interval:</u>
The hypothetical mean is 1.0000
The actual mean is 0.7000
The difference between these two values is -0.3000
The 95% confidence interval of this difference:
From -0.3194 to -0.2806

<u>Intermediate values used in calculations:</u>

t = 31.7490
df = 27
standard error of difference = 0.009

It is concluded that when comparing the MCNP neutron results against the Attila™ calculated results we can reject the null hypothesis that the underlying mean ratio is 1.0. Furthermore, an examination of the data reveals that the MCNP results are consistently between 20% and 40% lower when compared to the Attila™ results. This strongly suggests that the Attila™ and MCNP models may be fundamentally different from each other.

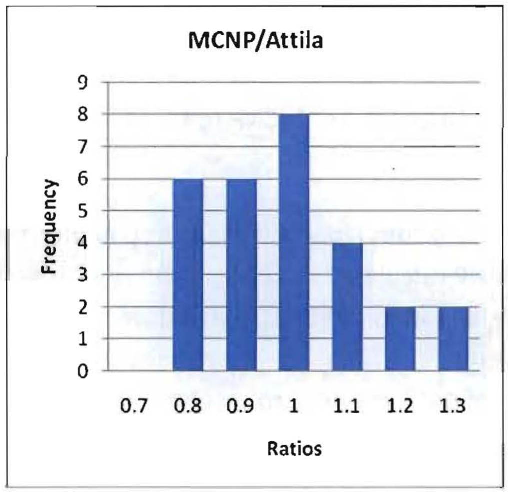

Figure 19 – Histogram of MCNP to Attila™Neutron Ratios

7 CONCLUSION

The primary focus of this evaluation was to explore Attila's CAD import capability as a means to reduce the time and cost to evaluate new designs for compliance with worker dose regulations; and, to evaluate Attila's ability to yield accurate results.

This evaluation confirms Attila's stated ability to import CAD models and use them to generate accurate results. While the CAD import process requires some up-front work, it is functional and could reduce the cost of design analysis in the long run.

7.1 CAD Import Process

The CAD model's level of complexity bears upon the success of the import process. Models with high degrees of complexity, numerous parts, and those containing small rounded annular components may create difficulties to the analyst's importing effort. In general it can be stated that Attila™ has an affinity for non-rounded shapes and an aversion to the opposite. Models that minimize problematic shapes import accurately and with ease.

The CAD model used in this evaluation contained many of the shapes that create problems for the import process. For this reason, and because the analyst was learning to use of the software, the import process did not prove to be as efficient as was expected. Once the analyst learned how to examine the model for problematic shapes and fix their geometry, the process ran well.

The lesson learned in the import process is that a CAD model needs some up-front work to enable a smooth and efficient import process. Unnecessary components should be eliminated. Rounded components should be carefully examined and substituted, if feasible, with a non rounded counterpart. For example, consider Figure 20. The two shapes are actually one and the same. The shape on the right is drawn showing shades and edges. It is made from a 32 sided polygon. Substituting a polygon for the rounded small annular shape will not impact the model's results. It will however, make the CAD import and subsequent mesh creation simpler.

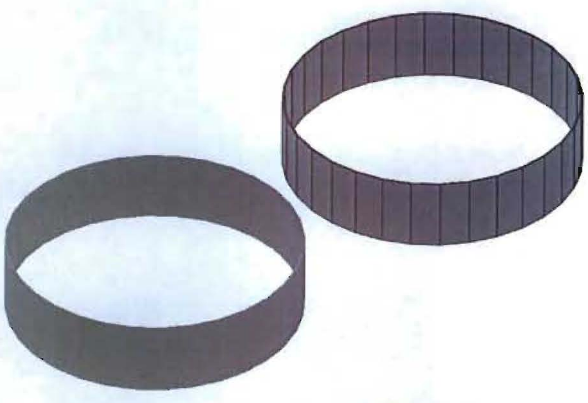

Figure 20 – Polygon Substitution

These kinds of modifications to a candidate CAD model should be done by a CAD specialist. The efficiency sought would largely disappear if these modifications were to be done by the dose modeling analyst. This constitutes an additional scope of work for the engineering team that needs careful consideration.

One of the goals of creating an MCNP model during this evaluation was to demonstrate that simple geometry can produce good results. The simplistic MCNP model created to explore this theory produced photon results that were not statistically different from measured results. On the other hand, the systematic bias between Attila™ and MCNP neutron calculations is of concern and suggests that the MCNP model, particularly the source shape and density, should be further developed.

In conclusion, the Attila™ import process using solid objects could reduce the time and cost to evaluate new designs provided that up-front work is done to the CAD model to eliminate unnecessary components and to modify problematic shapes.

7.2 Attila's Calculated Results

The results clearly indicate that Attila™ is accurate in assessing radiation flux given an accurate representation of the source term and geometry. This was not an unexpected result as there are many published benchmark tests confirming this conclusion.

For the case of photon results, Attila's results were not statistically distinguishable from the measured results. For the case of neutron results, Attila's results were comparable to the few measured results that were useful.

Attachment 1 – Neutron Spectral Data

Energy Bin (MeV)		Intensity (dps)
0.00E+00	7.00E-01	1.24E+01
7.00E-01	1.40E+00	1.53E+01
1.40E+00	2.10E+00	1.23E+01
2.10E+00	2.80E+00	8.69E+00
2.80E+00	3.50E+00	5.70E+00
3.50E+00	4.20E+00	3.55E+00
4.20E+00	4.90E+00	2.14E+00
4.90E+00	5.60E+00	1.25E+00
5.60E+00	6.30E+00	7.14E-01
6.30E+00	7.00E+00	4.01E-01
7.00E+00	7.70E+00	2.22E-01
7.70E+00	8.40E+00	1.21E-01
8.40E+00	9.10E+00	6.52E-02
9.10E+00	9.80E+00	3.48E-02
9.80E+00	1.05E+01	1.84E-02
1.05E+01	1.12E+01	9.63E-03
1.12E+01	1.19E+01	5.01E-03
1.19E+01	1.26E+01	2.59E-03
1.26E+01	1.33E+01	1.33E-03
1.33E+01	1.40E+01	6.79E-04

Attachment 2 – Photon Input Spectral Data

Energy Bin (MeV)		Intensity (dps)
0.000	0.013	0.000E+00
0.013	0.014	4.232E+06
0.014	0.025	7.190E+06
0.025	0.027	2.919E+05
0.027	0.031	2.260E+03
0.031	0.034	1.668E+04
0.034	0.043	2.332E+05
0.043	0.046	2.611E+05
0.046	0.051	1.774E+04
0.051	0.059	6.141E+05
0.059	0.060	4.364E+06
0.060	0.068	5.886E+03
0.068	0.071	5.462E+03
0.071	0.079	1.366E+04
0.079	0.096	9.082E+04
0.096	0.105	2.966E+05
0.105	0.112	5.141E+04
0.112	0.122	6.242E+04
0.122	0.130	1.387E+05
0.130	0.141	6.511E-01
0.141	0.160	1.082E+04
0.160	0.200	1.658E+04
0.200	0.210	5.050E+04
0.210	0.250	1.884E+03
0.250	0.300	4.762E+03

Energy Bin (MeV) (Continued)		Intensity (dps)
0.250	0.300	4.762E+03
0.300	0.330	2.339E+03
0.330	0.370	3.332E+04
0.370	0.400	5.826E+04
0.400	0.450	3.515E+04
0.450	0.520	4.284E+03
0.520	0.580	1.719E+01
0.580	0.600	4.657E+00
0.600	0.640	2.426E+02
0.640	0.680	1.073E+03
0.680	0.750	2.488E+02
0.750	0.850	3.764E+02
0.850	0.980	1.187E+01
0.980	1.100	3.134E+00
1.100	1.240	2.828E-08
1.240	1.300	1.759E-09
1.300	1.500	1.118E-08
1.500	1.600	6.186E-09
1.600	1.700	1.898E-09
1.700	1.900	2.808E-08
1.900	2.300	8.310E-09
2.300	2.620	1.813E-09
2.620	3.000	1.484E-10
3.000	4.000	3.562E-11